Journal of Zhejiang University-SCIENCE B (Biomedicine & Biotechnology) in press
www.jzus.zju.edu.cn; www.springer.com/journal/11585
E-mail: jzus_b@zju.edu.cn

Correspondence

https://doi.org/10.1631/jzus.B2500519

Spatial transcriptomic profiling reveals subtype-specific ecosystems in human esophageal sarcomatoid carcinoma: two rare case reports

Lei GAO[1*], Yao CHEN[2*], Xinyu MEI[1✉], Jieyong TIAN[1✉]

[1]*Department of Thoracic Surgery, The First Affiliated Hospital of USTC, Division of Life Sciences and Medicine, University of Science and Technology of China, Hefei, Anhui Province, 230001, China*
[2]*Department of Pathology, The First Affiliated Hospital of USTC, Division of Life Sciences and Medicine, University of Science and Technology of China, Hefei, Anhui Province, 230001, China*

Esophageal sarcomatoid carcinoma (ESC) is a rare and aggressive malignancy, representing only 0.2% to 2% of all human esophageal cancers. Histologically, ESC is characterized by biphasic appearance of both carcinomatous (typically squamous) and sarcomatoid components (Raza and Mazzara, 2011; Ajani et al., 2023). The variable proportion of malignant components within the tumor region can further define several histologic subtypes such as sarcomatoid-dominant and carcinomatous-dominant ESC (Raza and Mazzara, 2011). Treatment options for ESC patients are exactly like those established for conventional esophageal cancers, which rely on surgery-based multimodal strategies including neoadjuvant chemoradiation and adjuvant therapies after surgery (Ajani, et al., 2023). Nevertheless, the prognosis for ESC patients remains poor due to the frequent recurrence and early metastasis driven by its malignant potential (Hashimoto et al., 2019). Due to the rarity of human ESC, both fundamental research and clinical trials are greatly constrained. Systematic analysis of the cellular and molecular mechanisms underlying ESC pathogenesis would provide the foundational framework needed for developing efficient therapeutics against this malignancy (Raza and Mazzara, 2011).

In the present study, to determine the cellular and molecular characteristics of human ESC at high resolution, two ESC patients were enrolled for spatial transcriptomic profiling (Fig. 1a). They visited our outpatient department for the evaluation of dysphagia and were diagnosed with esophageal malignant cancer. Both patients were classified as clinical stage II (cT3N0M0 for Patient 1 and cT2N0M0 for Patient 2) and underwent minimally invasive McKeown esophagectomy (Fig. 1b). Histologic examinations confirmed the diagnosis of ESC in both patients (Figs. S1a-d). The pathological stage was IIA (pT2N0M0) for Patient 1 (14 lymph nodes dissected without metastasis) and IIB (pT1bN1M0) for Patient 2 (28 lymph nodes dissected with metastasis identified in one paraoesophageal metastasis).

To remove potential batch effects between the two samples, we first integrated processed spatial transcriptomic data with a defined Seurat workflow (Fig. S1e). Unsupervised clustering of spots generated

✉ Xinyu MEI, mxyahslyy@ustc.edu.cn
✉ Jieyong TIAN, tjyong77@sina.cn
* The two authors contributed equally to this work
Lei GAO, https://orcid.org/0000-0003-3948-9213
Xinyu MEI, https://orcid.org/0000-0003-4272-216X
Jieyong TIAN, https://orcid.org/0009-0003-9025-269X

Received Aug. 25, 2025; Revision accepted Dec. 6, 2025;
Crosschecked xxx. xx, 20xx; Published online xxx. xx, 20xx

seven distinct cell populations (Fig. S1f) with differentially expressed genes (DEGs) (Fig. S1g). To define the identity of these cell populations, we also used non-negative matrix factorization (NMF) analysis, an unsupervised learning algorithm for niche extraction (Franzén et al., 2024). A total of 22 NMF factors were automatically identified (Fig. S2a), and functional enrichment for the factors was generated (Fig. S2b). On the basis of Pearson correlation analysis, the authentic identity of these cell populations was found to be as expected and was annotated (Fig. 1c). In Patient 1, the tumor region was predominantly composed of three transcriptionally and spatially distinct sarcomatoid components. In contrast, the tumor region in Patient 2 primarily consisted of squamous tissue, with a small proportion of sarcomatoid infiltration (Figs. 1d and 1e). While these sarcomatoid components were functionally distinct, the squamous-cell-carcinoma component exhibited pronounced homogeneity (Fig. 1f). Compared with Patient 1 (sarcomatoid-dominant ESC), a much higher cellular heterogeneity was found in Patient 2 (squamous-dominant ESC), as evidenced by the number of cell populations (Fig. 1g). Collectively, these findings indicate that these two ESC subtypes are largely distinct in terms of cellular composition and function.

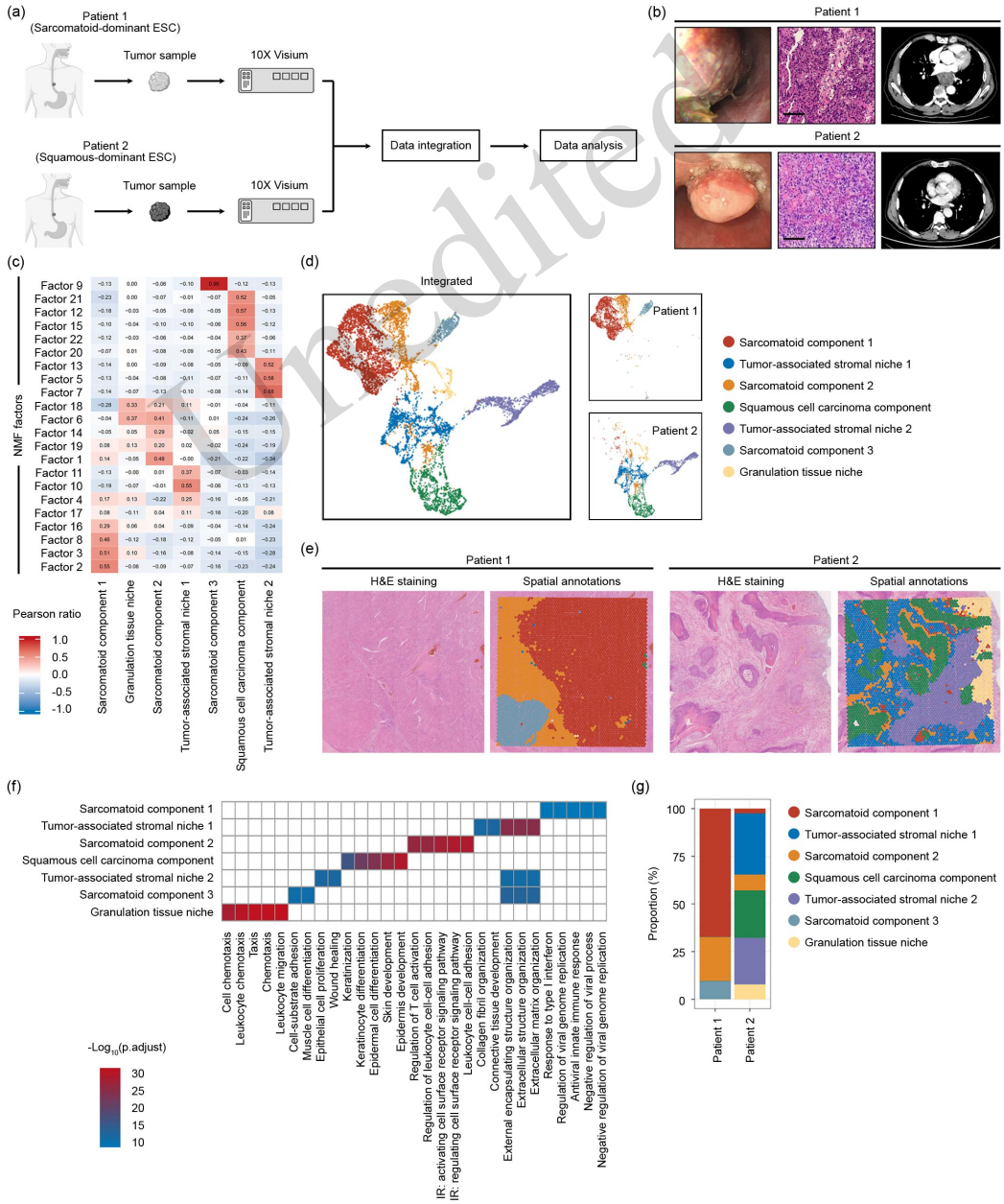

Fig. 1 Spatial transcriptomic characterization of human ESC. (a) Schematic of the study design. (b) Endoscopic, H&E-stained, and contrast-enhanced CT images of esophageal tumors in two ESC patients before surgery. Scale bar, 200 μm. (c) Pearson correlation heatmap of NMF factors and inferred cell types across all spots. UMAP (d) and in situ visualization of spot clusters (e) obtained from two ESC patients. Spots are colored based on cell population. (f) Heatmap showing top enriched biological processes for each cell population. (g) Proportion of cell populations in two ESC patients.

To examine the difference in cell-lineage distribution between ESC subtypes in an unbiased manner, we used SpaCET, an algorithm designed for automatically estimating cell lineages within the malignant tumor microenvironment (Ru et al., 2023). Both subtypes were composed of malignant cells and cancer-associated fibroblasts, but squamous-dominant ESC showed increased immune-cell infiltration that was spatially restricted in the malignant niches (Fig. S3). To further characterize differences in immune-cell infiltration between ESC subtypes, we isolated immune-cell-enriched spots with high *PTPRC* expression and performed cell clustering (Figs. S4a-S4e). The immune-cell landscape in sarcomatoid-dominant ESC was dominated by antigen-presenting dendritic cells and lymphoid linages including plasma and B cells. In contrast, squamous-dominant ESC showed prominent infiltration of innate immune cells, including macrophages and neutrophils (Fig. S4f). The efficacy of immunotherapy in neoadjuvant and consolidation treatment of esophageal malignancy has been established (Wang et al., 2024). We next quantitatively compared the expression of defined immune targets (both checkpoint and co-stimulatory molecules) in the two ESC subtypes. Our findings revealed that key immune checkpoints such as *CTLA4* (encoding CTLA-4), *PDCD1* (encoding PD-1), and *CD274* (encoding PD-L1) were markedly upregulated in sarcomatoid-dominant ESC. In contrast, only *LAG3* (encoding LAG-3) and *VSIR* (encoding B7-H5) were substantially elevated in squamous-dominant ESC (Fig. S5). In addition, these co-stimulatory molecules displayed distinct expression patterns in each subtype. These findings thus suggest that these two ESC subtypes exhibit distinctive immune-cell infiltration features and therapeutic vulnerabilities.

Differential expression analysis further revealed subtype-specific upregulated differentially expressed genes (DEGs) (Fig. 2a). Functional enrichment results indicated that sarcomatoid-dominant ESC-specific upregulated DEGs were highly enriched in adoptive immune response processes; squamous-dominant ESC-specific upregulated DEGs were largely enriched in extracellular organization processes (Fig. 2b). To uncover the upstream regulators underlying ESC subtype-specific gene-expression programs, we carried out transcription factor (TF) activity inference with the decouple algorithm (Badia et al., 2022). Subtype-specific activated TFs and their downstream target genes were identified and subsequently overlapped with subtype-upregulated genes. Consistently, active TFs in sarcomatoid-dominant ESC appeared to drive immune-related signaling, whereas those in squamous-dominant ESC mainly governed programs involved in epithelial-cell proliferation and differentiation (Fig. S6). By inferring copy number alteration (Erickson et al., 2022), we were able to identify substantial malignant potential in both histologic subtypes (Fig. S7a). The most fundamental trait of malignant cells is their ability to sustain persistent proliferation (Hanahan and Weinberg, 2011). We then quantitatively compared the proliferation potential of the ESC subtypes. The proliferation score was much higher in cell populations of squamous-dominant ESC (Figs. 2c and S7b). The ratio of Ki-67 positive cells was also consistently quite high in squamous-dominant ESC (Fig. 2d). In addition, type 3 sarcomatoid tissue was identified as a terminal state in sarcomatoid-dominant ESC, but in squamous-dominant ESC, both type 1 and 2 sarcomatoid tissue was differentiated from the squamous component (Figs. 2e and S7c). The enhanced proliferative and differentiation capacity of squamous-dominant ESC is indicative of a more aggressive tumor phenotype. To further evaluate this, we quantitatively compared oncogenic pathway activity between the subtypes (Sanchez-Vega et al., 2018). As shown in Fig. 2f, the activity of all pathways except canonical Wnt signaling was significantly increased in squamous-dominant ESC, reinforcing its more aggressive phenotype. Finally, component-specific differential analysis (Fig. 2g) further revealed the functional divergence between the subtypes. While sarcomatoid-component-specific genes were highly enriched in immune-response events, squamous-component-specific genes were largely enriched in keratinization processes (Fig. 2h). Collectively, these results reveal that two human ESC subtypes are functionally distinct.

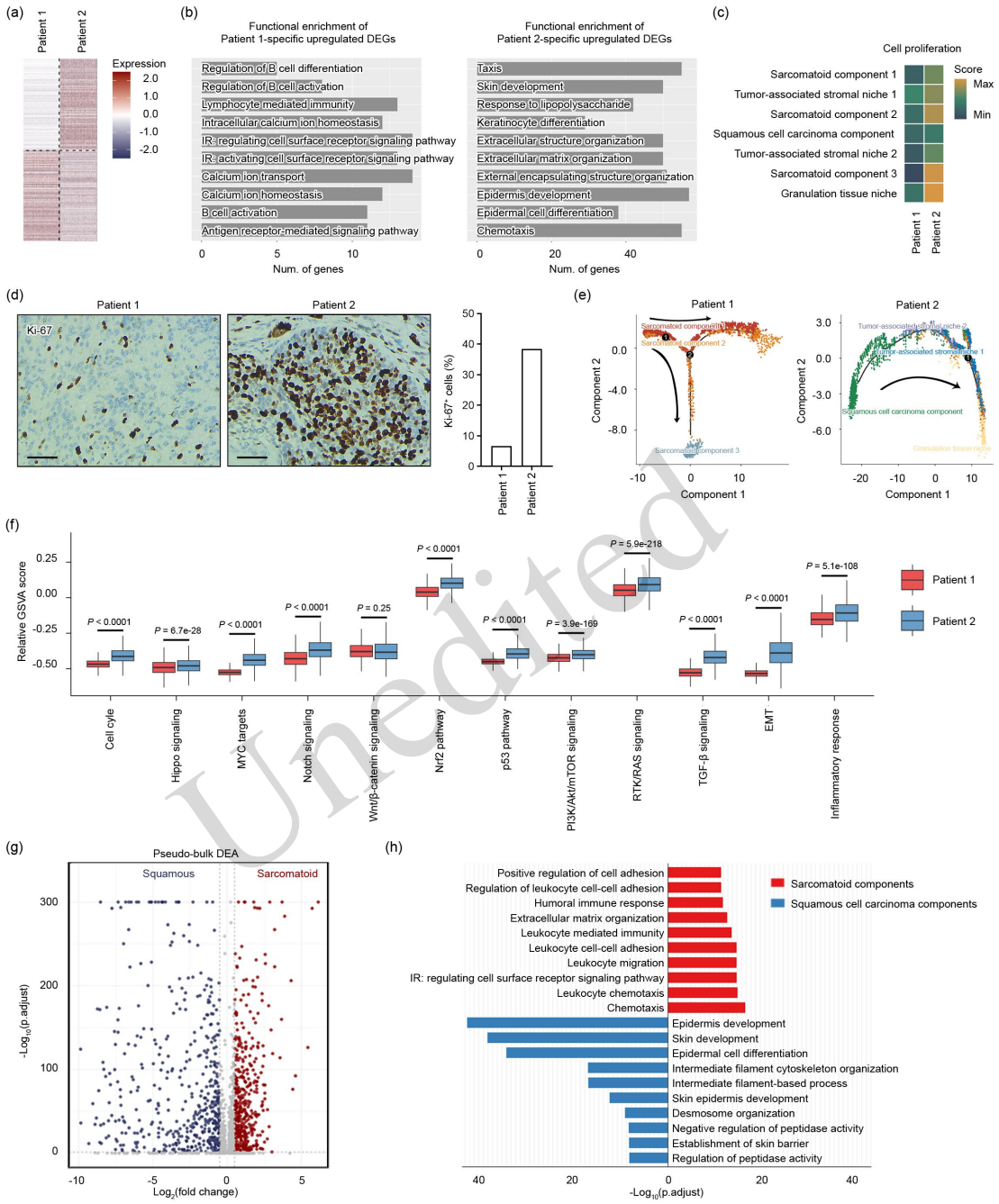

Fig. 2 Functional heterogeneity between human ESC subtypes. (a) Heatmap showing DEGs significantly expressed in each ESC subtype. (b) Bar plots showing top enriched biological processes for ESC subtype-specific upregulated DEGs. (c) Heatmap showing the enrichment score of the specified gene set across cell populations in both ESC subtypes. (d) Representative immunohistochemical staining of Ki-67 with quantitative data provided. Scale bar, 100 μm. (e) Monocle 2-inferred trajectory analysis of spots from each ESC subtype, colored based on cell population. (f) Relative GSVA score of the oncogenic signaling pathways between two ESC subtypes. P values were calculated using two-tailed unpaired Student's t-tests. (g) Volcano plot showing upregulated DEGs in the ESC subtypes. (h) Bar plot showing top enriched biological processes of component-specific upregulated DEGs.

In conclusion, this study provides the first high-resolution evidence that human sarcomatoid-dominant and squamous-dominant ESC subtypes represent distinct biological entities. The malignant potential and prognosis of ESC have been previously characterized (Handra-Luca et al., 2001; Raza and Mazzara, 2011; Hashimoto, et

al., 2019); however, the functional divergence between histologic subtypes remains elusive. On the basis of our prior application of omics platforms in analyzing diseases (Gao et al., 2021; Gao et al., 2023), we employed spatial transcriptomics to uncover fundamental differences in cellular composition and functional states between ESC subtypes. The squamous component exhibits pronounced transcriptional homogeneity, whereas sarcomatoid components display substantial cellular heterogeneity. By constructing the cell-differentiation trajectory (Zhang et al., 2022), we also identified sarcomatoid tissue as the terminal differentiation state, supporting the hypothesis that sarcomatoid tissue could be derived from metaplasia of squamous carcinoma cells via an epithelial-mesenchymal transition mechanism (Raza and Mazzara, 2011). As the most distinctive feature of malignancy, the proliferative potential of malignant cells mediates tumor growth and metastasis (Hanahan and Weinberg, 2011; El-Tanani et al., 2024). Proliferation capacity also differs between ESC subtypes, with the squamous-dominant variety exhibiting highly increased proliferation activity. Due to the remarkable differentiation potential of squamous-dominant ESC, this subtype can be more aggressive, as shown by its broadly elevated oncogenic pathway activity. For these patients, consolidation chemotherapy and/or immunotherapy, combined with surveillance, should be prioritized to mitigate the recurrence risk. In addition, the distinct immune-cell infiltration and differential expression patterns of immune-checkpoint and co-stimulatory molecules of the ESC subtypes could indicate immunotherapeutic susceptibility. Thus, we highly recommend comprehensive molecular profiling of immune targets in ESC to guide subtype-specific therapeutic strategies and improve clinical outcomes. This report represents an in-depth study of only two paired patients, with findings that need to be extended to a larger cohort of ESC patients. While the biological distinctions we found are robust for these individual cases, their generalizability across the broader ESC patients remains provisional. What we provide here is a definitive high-resolution framework and testable hypotheses regarding subtype-specific pathogenesis. Nevertheless, this study suggests that a spatial omics-based approach could be a powerful tool for deconvoluting ESC pathogenesis and also provide a reference atlas for its mechanistic dissection.

Data availability statement

The data supporting this study are available from the corresponding authors upon reasonable request. The data reported in this paper have been deposited in the OMIX, China National Center for Bioinformation/Beijing Institute of Genomics, Chinese Academy of Sciences (https://ngdc.cncb.ac.cn/omix: accession no. OMIX013513). The present study does not generate any new code; the code used in the present study is provided in the supplementary data.

Declaration on the Use of Generative AI Tools

No generative AI tools were used in the preparation of this manuscript.

Acknowledgments

This work was supported by the National Natural Science Foundation of China (82100266, 82570092) and the Natural Science Research Project of Anhui Education Committee (2024AH052055, 2024AH040256). We sincerely thank the two patients for their tissue donations.

Author contributions

Jieyong TIAN and Xinyu MEI supervised the project and conceived the study. Lei GAO and Yao CHEN performed all experiments and analyses. Lei GAO wrote the manuscript; Jieyong TIAN and Xinyu MEI revised the manuscript.

Compliance with ethics guidelines

Lei GAO, Yao CHEN, Xinyu MEI, and Jieyong TIAN declare that they have no conflict of interest.

All procedures followed were in accordance with the ethical standards of the responsible committee on human experimentation (institutional and national) and with the Helsinki Declaration of 1975, as revised in 2008. Human ESC tumor samples and histologic images were obtained with an approval by the Ethics Committee of The First Affiliated Hospital of University of Science and Technology of China (2024-RE-374).

References

Ajani JA, D'amico TA, Bentrem DJ, et al., 2023. Esophageal and esophagogastric junction cancers, version 2.2023, nccn clinical practice guidelines in oncology. *J Natl Compr Canc Netw*, 21(4):393-422. https://doi.org/10.6004/jnccn.2023.0019

Badia IMP, Vélez Santiago J, Braunger J, et al., 2022. Decoupler: Ensemble of computational methods to infer biological activities from omics data. *Bioinform Adv*, 2(1):vbac016. https://doi.org/10.1093/bioadv/vbac016

El-Tanani M, Rabbani SA, Babiker R, et al., 2024. Unraveling the tumor microenvironment: Insights into cancer metastasis and therapeutic strategies. *Cancer Lett*, 591:216894. https://doi.org/10.1016/j.canlet.2024.216894

Erickson A, He M, Berglund E, et al., 2022. Spatially resolved clonal copy number alterations in benign and malignant tissue. *Nature*, 608(7922):360-367. https://doi.org/10.1038/s41586-022-05023-2

Franzén L, Olsson Lindvall M, Hühn M, et al., 2024. Mapping spatially resolved transcriptomes in human and mouse pulmonary fibrosis. *Nat Genet*, 56(8):1725-1736. https://doi.org/10.1038/s41588-024-01819-2

Gao L, Zhang H, Cui J, et al., 2021. Single-cell transcriptomics of cardiac progenitors reveals functional subpopulations and their cooperative crosstalk in cardiac repair. *Protein Cell*, 12(2):152-157. https://doi.org/10.1007/s13238-020-00788-6

Gao L, Sun Y, Zhang X, et al., 2023. Wnt3a-loaded extracellular vesicles promote alveolar epithelial regeneration after lung injury. *Adv Sci (Weinh)*, :e2206606. https://doi.org/10.1002/advs.202206606

Hanahan D, Weinberg RA, 2011. Hallmarks of cancer: The next generation. *Cell*, 144(5):646-674. https://doi.org/10.1016/j.cell.2011.02.013

Handra-Luca A, Terris B, Couvelard A, et al., 2001. Spindle cell squamous carcinoma of the oesophagus: An analysis of 17 cases, with new immunohistochemical evidence for a clonal origin. *Histopathology*, 39(2):125-132. https://doi.org/10.1046/j.1365-2559.2001.01174.x

Hashimoto M, Kitagami H, Niwa H, et al., 2019. Prognosis and prognostic factors of esophageal spindle cell carcinoma treated by esophagectomy: A retrospective single-institution analysis. *Esophagus*, 16(3):292-299. https://doi.org/10.1007/s10388-019-00667-y

Raza MA, Mazzara PF, 2011. Sarcomatoid carcinoma of esophagus. *Arch Pathol Lab Med*, 135(7):945-948. https://doi.org/10.5858/2010-0074-rsr.1

Ru B, Huang J, Zhang Y, et al., 2023. Estimation of cell lineages in tumors from spatial transcriptomics data. *Nat Commun*, 14(1):568. https://doi.org/10.1038/s41467-023-36062-6

Sanchez-Vega F, Mina M, Armenia J, et al., 2018. Oncogenic signaling pathways in the cancer genome atlas. *Cell*, 173(2):321-337.e310. https://doi.org/10.1016/j.cell.2018.03.035

Wang X, Kang X, Zhang R, et al., 2024. Chemoradiotherapy and subsequent immunochemotherapy as conversion therapy in unresectable locally advanced esophageal squamous cell carcinoma: A phase ii nexus-1 trial. *Clin Cancer Res*, 30(22):5061-5072. https://doi.org/10.1158/1078-0432.Ccr-24-1236

Zhang B, Zhang F, Lu F, et al., 2022. Reduced cell invasion may be a characteristic of placental defects in pregnant women of advanced maternal age at single-cell level. *J Zhejiang Univ Sci B*, 23(9):747-759. https://doi.org/10.1631/jzus.B2101024

Supplementary information

Materials and methods; Figs. S1-S7